# EMI SHIELDING EFFECTIVENESS OF GRAPHENE NANOCOMPOSITES:EFFECTS OF FILLER LOADING AND THICKNESS

Sima Kashi[1], Vishak Perumal[2] and Russell Varley[1]

[1]Institute for Frontier Materials, Deakin University, Waurn Ponds, VIC 3216, Australia
Email: sima.kashi@deakin.edu.au, russell.varley@deakin.edu.au
[2]School of Engineering (Chemical), RMIT University, Melbourne, VIC 3000, Australia
Email: vishak.perumal@gmail.com

**Keywords:** EMI shielding, Graphene, Nanocomposite, Thickness effect

**Abstract**
The excellent physical properties of graphene can be exploited to both reinforce and give functionality to polymeric matrices such as electromagnetic interference (EMI) shielding. Incorporation of graphene in a polymer imparts electrical conductivity and permittivity to the matrix, and the nanocomposite can be used as a light-weight EMI shielding material. In the current study, graphene nanoplatelets were embedded in two polymers at different concentrations and the EMI shielding effectiveness of the nanocomposites were measured by using a vector network analyser and waveguide setup. Addition of graphene nanoplatelets enhanced the shielding performance of both polymers significantly. Furthermore, effect of sample thickness on shielding effectiveness of the nanocomposites was studied. Results showed that depending on the graphene content of the nanocomposite and frequency of radiation, increasing the sample thickness could either enhance the shielding performance of the sample or decrease its shielding effectiveness.

## 1. Introduction

Graphene-based polymeric nanocomposites have been investigated for a wide range of applications. The significant mechanical reinforcement obtained in graphene-based systems can be used in producing light-weight parts for automotive and aerospace applications. Addition of graphite oxide (GO) to polyamide 6 has also proved to result in nanocomposites with good short-term fire resistance [1]. Graphene-embedded polymers have also shown enhanced thermal stability and mechanical properties [2-4]. Graphene-based nanocomposites have been explored for biomedical applications such as in biosensors [5] and drug delivery systems [6] as well. However, due to the excellent electrical conductivity of graphene, the focus of many studies has been on applications of graphene-based nanocomposites in electronic and electrical devices. Energy storage devices [7] and solar cells [8] are among the areas where such materials can be used. Furthermore, these materials can be used in electrostatic discharge protection, lightening-protection panels, thermoelectric materials applications [9]. One of the areas where graphene-embedded polymers have shown promising results is in electromagnetic interference (EMI) shielding applications as viable light-weight replacement for the conventional metal-based shielding materials [9, 10]. Undesirable electromagnetic radiations are becoming a new source of pollution world-wide as a result of rapid increase in the use of electronic and telecommunication devices. Such radiations not only could interfere with function of other devices, they could also be a threat to human health [11, 12]. This critical issue drives the great demand for development of EMI shielding technology [13]. As a result, polymeric nanocomposites with electromagnetic properties are attracting attention as the next generation of efficient, light-weight and flexible EMI shielding materials [12, 14-16]. In the present study, we investigate the simultaneous effects of graphene nanoplatelets (GNP) loading and sample thickness on EMI shielding performance of two sets of nanocomposites with poly lactide and poly (butylene adipate-co-terephthalate) as the polymeric matrices. Morphology and rheological behavior of these systems have been reported previously [17-19].

## 2. Experimental

4032D grade PLA was purchased from NatureWorks LLC, having a density of 1.24 g/cm$^3$ and a melting temperature range of 155 - 170 °C. PBAT, under the catalogue name of Ecoflex F Blend C1200, was purchased from BASF. According to the technical data sheet, it has a density of 1.25–1.27 g/cm$^3$ and melting range of 110 - 120 °C. Grade M GNPs were obtained from XG Sciences (USA) with an average thickness of 6 - 8 nm, surface area of 120 - 150 m$^2$/g, density of 2.2 g/cm$^3$ and electrical conductivity of 10$^2$ and 10$^7$ S/m for perpendicular and parallel to the surface, respectively. GNPs were embedded in PLA and PBAT at six different concentrations of 0, 3, 6, 9, 12, and 15 wt% in an internal mixer at temperatures of 180 °C and 140 °C, respectively. The mixer was operated at 60 rpm with roller rotors for ten minutes. PLA/GNP and PBAT/GNP nanocomposites were then moulded using a hot press at a temperature of 180 °C and 140 °C, respectively, with a force of 80 kN for 5 min. Samples were coded as PL3, …, PL15 and PB3, …, PB15, where the number indicates the GNP content of the nanocomposite. Moulded samples of all the nanocomposites were prepared with two thickness of 1.5, and 2.8 mm and their EMI shielding effectiveness was determined via measuring their scattering (S-) parameters with a Wiltron vector network analyser (VNA) model 37269A over x-band frequency range (8.2-12.4 GHz).

## 3. Results and Discussion

EMI shielding is defined as the attenuation of electromagnetic radiation by reflection and/or absorption of the incident power [9]. When electromagnetic radiation ($P_I$) faces the shielding material, some of it will reflect back ($P_R$) and some will enter the material, which will be partially absorbed ($P_A$) and the rest will be transmitted ($P_T$) to the outer world.

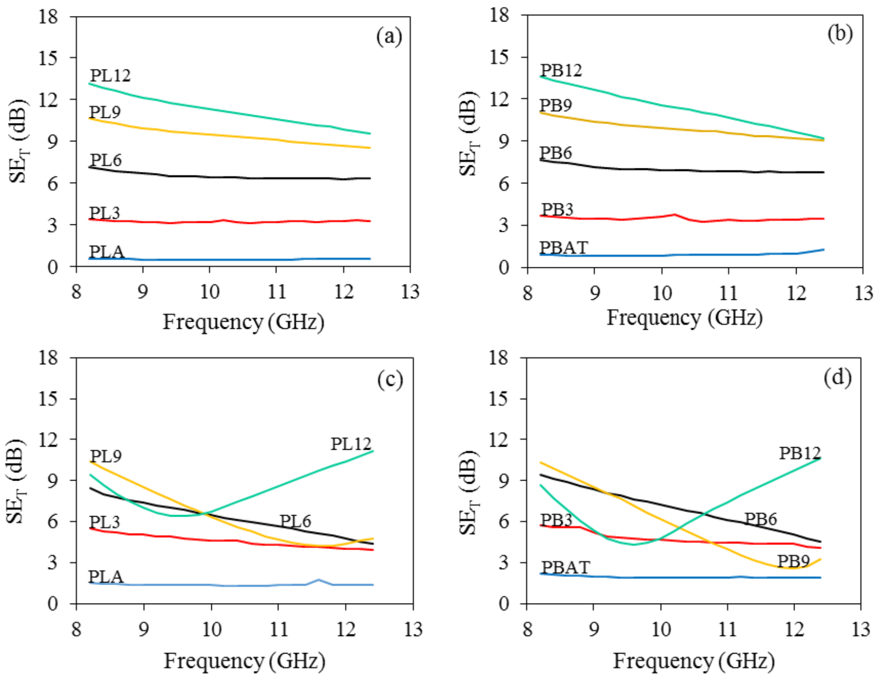


**Figure 1.** SE$_T$ of nanocomposites vs. frequency as a function of GNP loading; (a) PLA/GNP, 1.5 mm thick, (b) PBAT/GNP, 1.5 mm, (c) PLA/GNP, 2.8 mm and (d) PBAT/GNP, 2.8 mm.

Total shielding effectiveness ($SE_T$) of a material is the logarithmic ratio of the incident power to the transmitted power as in Eq. 1. Reflected and transmitted powers can be calculated from the S-parameters, measured by VNA, according to Eqs. 2-3. Efficiency of a material in attenuating EMI depends on frequency of radiation, thickness and electromagnetic properties of the material [20, 21]. Figure 1 depicts the $SE_T$ of PBAT/GNP and PLA/GNP nanocomposites as a function of GNP loading for two different thicknesses. It is observed in Figure 1(a,b) that with $SE_T$ of less than 1 dB, pure PLA and PBAT are transparent to the radiation. Addition of GNPs continuously increases the $SE_T$ of both polymers. This can be attributed to the enhancement of electrical conductivity and electrical permittivity of the polymers with GNP incorporation. For 1.5 mm thick samples in Figure 1(a,b), $SE_T$ of all nanocomposites with GNP loading of up to 9 wt% does not exhibit significant variations with frequency. However, a decreasing trend is observed in $SE_T$ behavior of PL12 and PB12.

$$SE_T = -10 \log (P_I/P_T) = 10 \log (1/T) \quad \text{, unit: decibels (dB)} \tag{1}$$

$$\text{Transmissivity } (T) = P_T/P_I = |S_{21}|^2 \quad \text{, no unit} \tag{2}$$

$$\text{Reflectivity } (R) = P_R/P_I = |S_{11}|^2 \quad \text{, no unit} \tag{3}$$

It is interestingly observed from Figure 1(c,d) that increasing the thickness of sample does not always result in higher $SE_T$. It can be seen that $SE_T$ of thicker samples have stronger frequency dependency and this dependency becomes stronger at higher GNP loadings. Considering PLA/GNP nanocomposites in Figure 1(a,c) for example, different trends are observed in variations of $SE_T$ with increasing thickness depending on the GNP content of the nanocomposite; for pure PLA and PL3, $SE_T$ increases with increasing sample thickness. For PL6, $SE_T$ of 2.8 mm sample exhibits much stronger frequency variations over 8.2-12.4 GHz frequency range compared to $SE_T$ of its 1.5 mm thick sample. The variations of $SE_T$ for PL9 and PL12 with thickness are more complex. The significant difference in frequency dependency of $SE_T$ behavior of pure polymers (similar to low GNP content nanocomposites) with thickness and that of highly filled polymers can be more clearly seen in Figure 2. Figure 1c shows that $SE_T$ of 2.8 mm thick samples of PL9 - PL12 go through a minimum as the frequency increases. With increasing GNPs from 9 to 12 wt% in the nanocomposites, this minimum shifts to lower frequencies. While $SE_T$ of 2.8 mm-thick PL12 is lower than $SE_T$ of 1.5 mm-thick PL12 over 8.2-11.8 GHz, it overtakes $SE_T$ of thin sample for frequencies above 11.8 GHz (Figure 2c). Similar observations can be made for PB9 and PB12 (Figure 1d and Figure 2d).

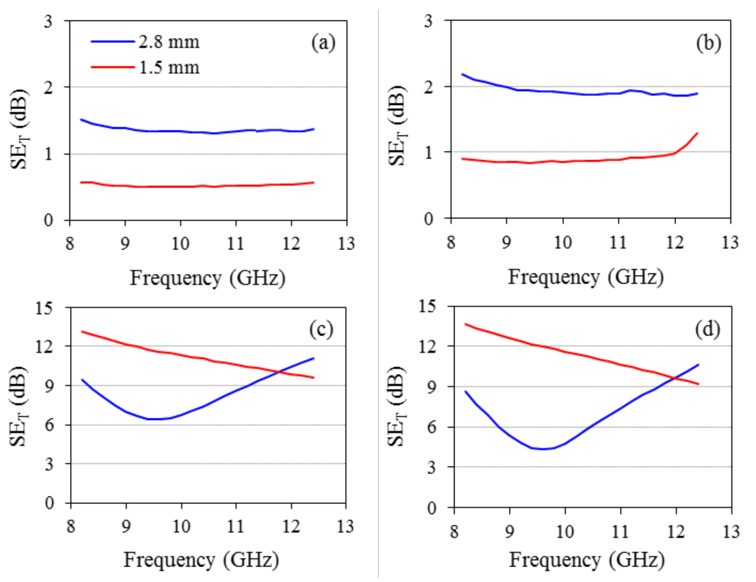


**Figure 2.** Effect of thickness on $SE_T$ behvaiour of (a) pure PLA, (b) pure PBAT, (c) PL12 and (d) PB12 samples with two different thickness.

Figure 3 illustrates the transmissivity and reflectivity of PLA/GNP and PBAT/GNP nanocomposites for 2.8 mm-thick samples. Pure polymers and nanocomposites with low GNP loading in Figure 3(a,b) have relatively constant T values versus frequency while at 6 wt%, T shows an increasing trend with increasing frequency from 8.2 to 12.4 GHz. Considering the reverse relation between $SE_T$ and T (Eq. 1), this explains the decreasing behavior of $SE_T$ of PL6 and PB6 in Figure 1(c,d) versus frequency. T values for 2.8 mm-thick samples of nanocomposites with 9 and 12 wt% GNPs have significant variations with frequency in Figure 3(a,b) and exhibit curves with maximum. As the GNP loading increases from 9 to 12 wt%, the peak in T becomes smaller and it occurs at lower frequencies. The reflectivities of the nanocomposites in Figure 3(c,d) exhibit trends opposite to those of their counterpart transmissivities in Figure 3(a,b). The peaks and dips in T and R, can be attributed to the multiple reflection phenomenon [22].

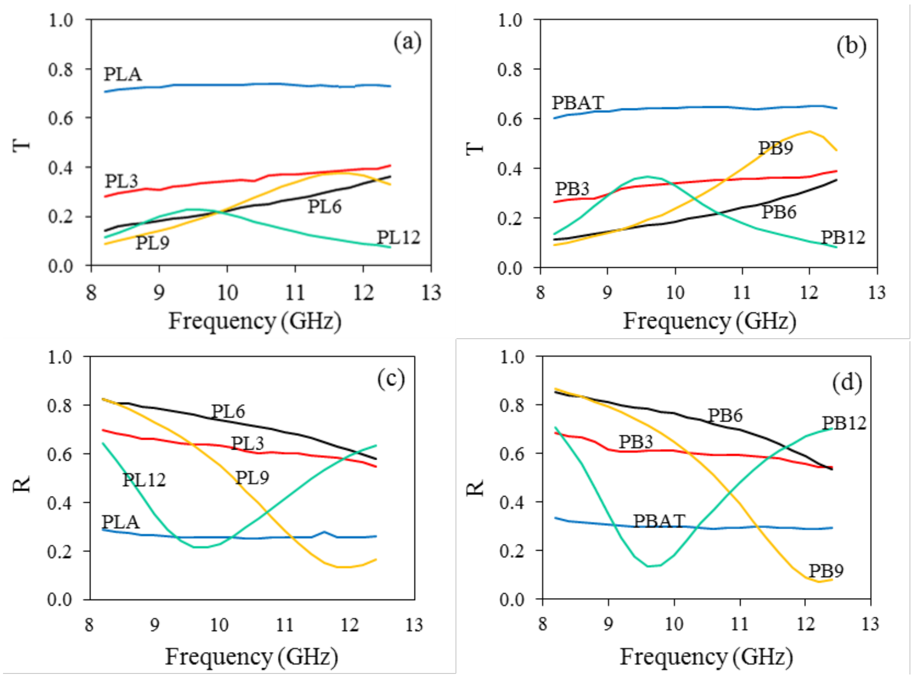


**Figure 3.** (a,b) Transmissivity and (c,d) reflectivity of PLA/GNP and PBAT/GNP nanocomposites vs. frequency for 2.8 mm-thick samples.

To better understand the effect of thickness on the EMI shielding effectiveness of the nanocomposites, their S-parameters were calculated (using the method of ref. [23]) at a fixed frequency of 10 GHz for the thickness range of 0 - 20 mm. Subsequently, T values were calculated and are illustrated in Figure 4 for pure polymers and nanocomposites with GNP content of 12 wt%. T of all samples show a general decreasing trend with periodic extremums (maximums and minimums) with increasing thickness. It is also observed that the fluctuations in T become smaller as the thickness increases from 0 to 20 mm. Furthermore, for highly filled nanocomposites (Figure 4 (c,d)), the fluctuations are found to dampen faster; it can be seen that T values of PL12 and PB12 do not vary appreciably with thickness for thicknesses above 10 and 16 mm, respectively. The fluctuations in the transmissivity behavior of the samples can be attributed to the multiple reflections of electromagnetic waves inside the shielding material. When the thickness of the nanocomposite is an even multiple of quarter wavelength of the wave inside the material, the multiple reflections have constructive effect on the T value and maximize it, minimizing the $SE_T$. On the other hand, when the thickness is an odd multiple of quarter wavelength of the wave in the material, multiple reflections affect the transmitted power in a destructive manner and minimize it and therefore maximizing $SE_T$ [24].

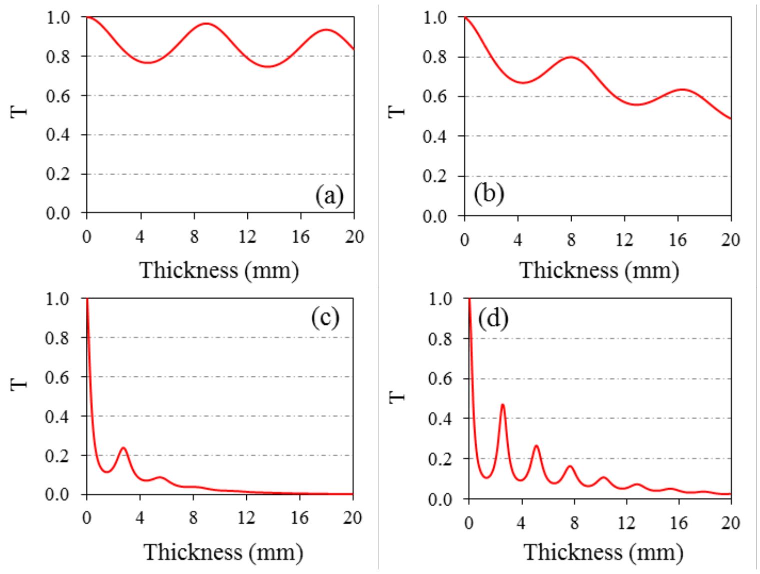


**Figure 4.** Calculated transmissivity of (a) pure PLA, (b) pure PBAT, (c) PL12 and (d) PB12 nanocomposites at fixed frequency (10 GHz) versus thickness.

## 4. Conclusions

The EMI shielding effectiveness of two series of nanocomposites was assessed over 8.2-12.4 GHz frequency range and the effects of filler loading and sample thickness on $SE_T$ of the nanocomposites was studied. Unmodified polymeric matrices were transparent to the electromagnetic radiations but addition of graphene nanoplatelets enhanced their $SE_T$ significantly. Increasing the thickness of nanocomposites samples from 1.5 mm to 2.8 mm showed that thicker samples do not necessary have higher $SE_T$ values. Calculations revealed a periodic behavior in the transmissivity of samples versus thickness, which explained the minimum SET values observed for 2.8 mm-thick highly filled nanocomposites.

## Acknowledgments

Authors would like to acknowledge the support received from the Australian Research Council (ARC) Research Hub for Future Fibres (IH140100018) funded by the Australian Government for presenting this work at the 18th European Conference on Composite Materials (ECCM18).

## References

[1] A. Dasari, Z.-Z. Yu, Y.-W. Mai, G. Cai, H. Song, Roles of graphite oxide, clay and POSS during the combustion of polyamide 6, *Polymer* 50(6) (2009) 1577-1587.
[2] S. Kashi, R.K. Gupta, N. Kao, S.A. Hadigheh, S.N. Bhattacharya, Influence of graphene nanoplatelet incorporation and dispersion state on thermal, mechanical and electrical properties of biodegradable matrices, *Journal of Materials Science & Technology* (2017).
[3] S. Kashi, R. Gupta, N. Kao, S. Bhattacharya, Preparation and Characterization of Poly Lactide and Poly (Butylene Adipate-co-Terephthalate) Nanocomposites Reinforced with Graphene Nanoplatelet, *40th Annual Condensed Matter and Materials Meeting 2016*, Australian Institute of Physics, 2016, pp. 1-4.

[4] S. Kashi, R.K. Gupta, N. Kao, S.N. Bhattacharya, Rheology and physical characterization of graphene nanoplatelet/poly (butylene adipate-co-terephthalate) nanocomposites, *AIP Conference Proceedings, AIP Publishing*, 2017, p. 030004.

[5] J. Lu, I. Do, L.T. Drzal, R.M. Worden, I. Lee, Nanometal-decorated exfoliated graphite nanoplatelet based glucose biosensors with high sensitivity and fast response, *ACS nano* 2(9) (2008) 1825-1832.

[6] H. Bai, C. Li, X. Wang, G. Shi, A pH-sensitive graphene oxide composite hydrogel, *Chemical Communications* 46(14) (2010) 2376-2378.

[7] C.-P. Tien, H. Teng, Polymer/graphite oxide composites as high-performance materials for electric double layer capacitors, *Journal of Power Sources* 195(8) (2010) 2414-2418.

[8] N. Spitsina, A. Lobach, M. Kaplunov, Polymer/nanocarbon composite materials for photonics, *High Energy Chemistry* 43(7) (2009) 552-556.

[9] S. Kashi, R.K. Gupta, T. Baum, N. Kao, S.N. Bhattacharya, Morphology, electromagnetic properties and electromagnetic interference shielding performance of poly lactide/graphene nanoplatelet nanocomposites, *Materials & Design* 95 (2016) 119-126.

[10] S. Kashi, R.K. Gupta, T. Baum, N. Kao, S.N. Bhattacharya, Dielectric properties and electromagnetic interference shielding effectiveness of graphene-based biodegradable nanocomposites, *Materials & Design* 109 (2016) 68-78.

[11] Y.-J. Wan, P.-L. Zhu, S.-H. Yu, R. Sun, C.-P. Wong, W.-H. Liao, Ultralight, super-elastic and volume-preserving cellulose fiber/graphene aerogel for high-performance electromagnetic interference shielding, *Carbon* 115 (2017) 629-639.

[12] Y.-J. Wan, P.-L. Zhu, S.-H. Yu, R. Sun, C.-P. Wong, W.-H. Liao, Graphene paper for exceptional EMI shielding performance using large-sized graphene oxide sheets and doping strategy, *Carbon* 122 (2017) 74-81.

[13] M. Cao, C. Han, X. Wang, M. Zhang, Y. Zhang, J. Shu, H. Yang, X. Fang, J. Yuan, Graphene nanohybrids: excellent electromagnetic properties for the absorbing and shielding of electromagnetic waves, *Journal of Materials Chemistry C* 6(17) (2018) 4586-4602.

[14] J. Liu, H.-B. Zhang, Y. Liu, Q. Wang, Z. Liu, Y.-W. Mai, Z.-Z. Yu, Magnetic, electrically conductive and lightweight graphene/iron pentacarbonyl porous films enhanced with chitosan for highly efficient broadband electromagnetic interference shielding, *Composites Science and Technology* 151 (2017) 71-78.

[15] H. Yang, Z. Yu, P. Wu, H. Zou, P. Liu, Electromagnetic interference shielding effectiveness of microcellular polyimide/in situ thermally reduced graphene oxide/carbon nanotubes nanocomposites, *Applied Surface Science* 434 (2018) 318-325.

[16] S. Bi, L. Zhang, C. Mu, H.Y. Lee, J.W. Cheah, E.K. Chua, K.Y. See, M. Liu, X. Hu, A comparative study on electromagnetic interference shielding behaviors of chemically reduced and thermally reduced graphene aerogels, *Journal of colloid and interface science* 492 (2017) 112-118.

[17] S. Kashi, R.K. Gupta, T. Baum, N. Kao, S.N. Bhattacharya, Phase transition and anomalous rheological behaviour of polylactide/graphene nanocomposites, *Composites Part B: Engineering* 135 (2018) 25-34.

[18] S. Kashi, R.K. Gupta, N. Kao, S.N. Bhattacharya, Viscoelastic properties and physical gelation of poly (butylene adipate-co-terephthalate)/graphene nanoplatelet nanocomposites at elevated temperatures, *Polymer* 101 (2016) 347-357.

[19] S. Kashi, R.K. Gupta, N. Kao, S.N. Bhattacharya, Electrical, thermal, and viscoelastic properties of graphene nanoplatelet/poly (butylene adipate-co-terephthalate) biodegradable nanocomposites, *Journal of Applied Polymer Science* 133(27) (2016).

[20] B. Zhao, C. Zhao, R. Li, S.M. Hamidinejad, C.B. Park, Flexible, Ultrathin, and High-Efficiency Electromagnetic Shielding Properties of Poly(Vinylidene Fluoride)/Carbon Composite Films, *ACS applied materials & interfaces* 9(24) (2017) 20873-20884.

[21] L.-L. Wang, B.-k. Tay, K.-y. See, Z. Sun, L.-K. Tan, D. Lua, Electromagnetic interference shielding effectiveness of carbon-based materials prepared by screen printing, *Carbon* 47(8) (2009) 1905-1910.

[22] M.H. Al-Saleh, U. Sundararaj, Electromagnetic interference shielding mechanisms of CNT/polymer composites, *Carbon* 47(7) (2009) 1738-1746.

[23] S. Kashi , S.A. Hadigheh, R. Varley, Microwave Attenuation of Graphene Modified Thermoplastic Poly(Butylene adipate-co-terephthalate) Nanocomposites, *Polymers* (2018), DOI: 10.3390/polym10060582

[24] A. Amiet, Free space permittivity and permeability measurements at microwave frequencies, *Monash University*, *Dept. of Electrical and Computer Systems Engineering*, *Melbourne*, *Australia* 2003.